

Improved determination of B_K with staggered quarks

Taegil Bae,¹ Yong-Chull Jang,¹ Hwancheol Jeong,¹ Chulwoo Jung,² Hyung-Jin Kim,²
Jangho Kim,¹ Jongjeong Kim,¹ Kwangwoo Kim,¹ Sunghee Kim,¹ Weonjong Lee,¹ Jaehoon
Leem,¹ Jeonghwan Pak,¹ Sungwoo Park,¹ Stephen R. Sharpe,³ and Boram Yoon⁴
(SWME Collaboration)

¹*Lattice Gauge Theory Research Center, FPRD, and CTP,*

Department of Physics and Astronomy, Seoul National University, Seoul, 151-747, South Korea

²*Physics Department, Brookhaven National Laboratory, Upton, NY11973, USA*

³*Physics Department, University of Washington, Seattle, WA 98195-1560, USA*

⁴*Los Alamos National Laboratory, Theoretical Division T-2, MS B283, Los Alamos, NM 87545, USA*

(Dated: April 4, 2021)

We present results for the kaon mixing parameter B_K obtained using improved staggered fermions on a much enlarged set of MILC asqtad lattices. Compared to our previous publication, which was based largely on a single ensemble at each of the three lattice spacings $a \approx 0.09$ fm, 0.06 fm and 0.045 fm, we have added seven new fine and four new superfine ensembles, with a range of values of the light and strange sea-quark masses. We have also increased the number of measurements on one of the original ensembles. This allows us to do controlled extrapolations in the light and strange sea-quark masses, which we do simultaneously with the continuum extrapolation. This reduces the extrapolation error and improves the reliability of our error estimates. Our final result is $\hat{B}_K = 0.7379 \pm 0.0047(\text{stat}) \pm 0.0365(\text{sys})$.

PACS numbers: 11.15.Ha, 12.38.Gc, 12.38.Aw

Keywords: lattice QCD, B_K , CP violation

I. INTRODUCTION

The kaon B-parameter, B_K , is one of the important hadronic inputs into the unitary triangle analysis of flavor physics. Fully controlled, first-principles calculations are only available using lattice QCD, and consistent results utilizing several fermion discretizations have now been obtained [1–4]. For a recent review, see Ref. [5]. Among these results are those we have previously presented using improved staggered fermions for both valence and sea quarks [2, 6]. Here we provide a significant update of these results, in which the control of several sources of systematic error is markedly improved.

Our previous result (Ref. [2]) was based largely on a single gauge ensemble at each of three lattice spacings ($a \approx 0.045$, 0.06 and 0.09 fm—dubbed “ultrafine”, “superfine” and “fine” hereafter). These ensembles had approximately the same physical values for the light sea-quark mass (m_ℓ , the degenerate up and down mass) and the strange sea-quark mass (m_s), allowing a continuum extrapolation. Extrapolating m_ℓ and m_s to their physical values was not, however, possible using these ensembles. Instead, we used results from “coarse” ensembles ($a \approx 0.12$ fm), for which a range of values of m_ℓ was available, to argue that the extrapolations in m_ℓ and m_s would lead to only a small shift in B_K . These ensembles were too coarse, however, to be included in our continuum extrapolation.

The main improvements since Ref. [2] are the inclusion of many additional ensembles and an increase in the number of measurements on ensembles used previously. Specifically, we have added results on seven more fine and four more superfine ensembles, while more than

quadrupling the number of measurements on the previously used superfine ensemble. (See Table II below.) The main impact of these improvements is that we can now do a controlled extrapolation in m_ℓ and m_s , which we do simultaneously with the continuum extrapolation. This leads to better understood and, in most cases, numerically smaller systematic errors. It also removes the need to use the coarse ensembles, with the entire analysis now carried out using results from the three finest lattice spacings.

In this report, we refer to Refs. [6] and [2] for explanations of many technical details. Since those papers were published, several updates have appeared in conference proceedings, the most recent being Ref. [7]. This report is based on our final data set, and the result supersedes earlier ones.

II. DATA SAMPLE

The kaon B parameter B_K is defined as

$$B_K(\mu, R) = \frac{\langle K^0 | O_{\Delta S=2}(\mu, R) | \bar{K}^0 \rangle}{8f_K^2 M_K^2/3} \quad (1)$$

where R is the renormalization scheme in which the operator $O_{\Delta S=2} = \sum_\nu [\bar{s}\gamma_\nu(1 - \gamma_5)d][\bar{s}\gamma_\nu(1 - \gamma_5)d]$ is defined, with μ is the corresponding renormalization scale. The standard scheme used in phenomenology is the $\overline{\text{MS}}$ scheme with naive dimensional regularization (NDR) for γ_5 . We match our lattice-regulated operators to this scheme, usually called NDR, using one-loop matching factors from Ref. [8]. We use the ensembles generated by

TABLE I. MILC asqtad ensembles used to calculate B_K . am_ℓ and am_s are the masses, in lattice units, of the light and strange sea quarks, respectively. “ens” indicates the number of configurations on which “meas” measurements are made. Ensembles added since Ref. [2] are denoted **new** while that with improved statistics is denoted **update**. Note that the numbering of the ID tags for fine and superfine lattices does not follow the ordering of am_ℓ .

a (fm)	am_l/am_s	geometry	ID	ens \times meas	status
0.12	0.03/0.05	$20^3 \times 64$	C1	564×9	old
0.12	0.02/0.05	$20^3 \times 64$	C2	486×9	old
0.12	0.01/0.05	$20^3 \times 64$	C3	671×9	old
0.12	0.01/0.05	$28^3 \times 64$	C3-2	275×8	old
0.12	0.007/0.05	$20^3 \times 64$	C4	651×10	old
0.12	0.005/0.05	$24^3 \times 64$	C5	509×9	old
0.09	0.0062/0.0186	$28^3 \times 96$	F6	950×9	new
0.09	0.0124/0.031	$28^3 \times 96$	F4	1995×9	new
0.09	0.0093/0.031	$28^3 \times 96$	F3	949×9	new
0.09	0.0062/0.031	$28^3 \times 96$	F1	995×9	old
0.09	0.00465/0.031	$32^3 \times 96$	F5	651×9	new
0.09	0.0031/0.031	$40^3 \times 96$	F2	959×9	new
0.09	0.0031/0.0186	$40^3 \times 96$	F7	701×9	new
0.09	0.00155/0.031	$64^3 \times 96$	F9	790×9	new
0.06	0.0072/0.018	$48^3 \times 144$	S3	593×9	new
0.06	0.0054/0.018	$48^3 \times 144$	S4	582×9	new
0.06	0.0036/0.018	$48^3 \times 144$	S1	749×9	update
0.06	0.0025/0.018	$56^3 \times 144$	S2	799×9	new
0.06	0.0018/0.018	$64^3 \times 144$	S5	572×9	new
0.045	0.0028/0.014	$64^3 \times 192$	U1	747×1	old

the MILC collaboration with $N_f = 2+1$ flavors of asqtad staggered sea quarks and a Symanzik-improved gauge action [9]. For valence quarks, we use HYP-smearred staggered fermions [10]. The advantages of this mixed action set-up are explained in Ref. [6].

We use the MILC asqtad lattices listed in Table I. As already noted, the eleven extra ensembles compared to Ref. [2] allow us to control the continuum and sea-quark mass extrapolations with much greater confidence. To give a sense of the range of these parameters, we present in Table II values for a^2 , the light sea-quark pion mass ($\sqrt{L_P}$) and the mass of the unphysical flavor-non-singlet $\bar{s}s$ state composed of sea quarks ($\sqrt{S_P}$). We will extrapolate/interpolate to physical sea-quark masses using L_P and S_P , while simultaneously extrapolating a^2 to zero. We exclude the coarse ensembles from Table II as they are not used in the final extrapolation.

We see from Table II that both fine and superfine lattices have a substantial range of pion masses, in the former case reaching down almost to the physical value. The fine lattices also have two values for $\sqrt{S_P}$, allowing interpolation to the “physical” value, 0.6858 GeV [12]. For the continuum extrapolation, the relevant quantity for our action is a^2 , and we see that this varies by almost a factor of four.

Staggered fermions introduce an unwanted “taste” degree of freedom, with each lattice staggered flavor giv-

TABLE II. Values for a^2 , $\sqrt{L_P}$ and $\sqrt{S_P}$ on the MILC ensembles used for our chiral-continuum extrapolation. a is determined from the mass-dependent values for r_1/a obtained by the MILC collaboration [9, 11], together with $r_1 = 0.3117$ fm.

ID	$a^2(0.01\text{fm}^2)$	$\sqrt{L_P}(\text{MeV})$	$\sqrt{S_P}(\text{MeV})$
F6	0.673	350	598
F4	0.706	485	765
F3	0.708	422	766
F1	0.710	346	764
F5	0.710	294	751
F2	0.710	243	755
F7	0.710	248	596
F9	0.710	174	759
S3	0.348	440	694
S4	0.348	383	694
S1	0.346	314	696
S2	0.347	262	695
S5	0.348	222	691
U1	0.192	316	703

ing rise to four degenerate tastes in the continuum limit. This unwanted degeneracy is removed by the fourth-root prescription, and we assume that this leads to the correct continuum limit. The effect of this prescription, as well as that of using a mixed action, can be incorporated into a chiral effective theory describing the staggered fermion formulation: staggered chiral perturbation theory (SChPT) [6, 13–15]. In particular, we use SU(2) SChPT at next-to-leading order (NLO) to obtain the functional form needed for extrapolations in light quark masses and a^2 .

III. DATA ANALYSIS AND FITTING

We calculate $B_K(1/a, \text{NDR})$ on each ensemble following the method explained in Ref. [6], using multiple measurements on each configuration. For the valence d quarks we use the four masses (in lattice units) $am_x = am_s^{\text{nom}} \times \{0.1, 0.2, 0.3, 0.4\}$, where m_s^{nom} is a nominal strange quark mass which lies fairly close to the physical value. For coarse, fine, superfine and ultrafine ensembles we take $am_s^{\text{nom}} = 0.05, 0.03, 0.018$ and 0.014 , respectively. For the valence s quarks we use the three masses $am_y = am_s^{\text{nom}} \times \{0.8, 0.9, 1.0\}$. With these values we are extrapolating to the “physical” $\bar{d}d$ mass (158 MeV—the mass of a flavor-non-singlet $\bar{d}d$ state) using lattice valence pions with masses in the range $\sim 200 - 400$ MeV. For the valence s quark we are extrapolating from the range $\sim 550 - 620$ MeV to the “physical” value 686 MeV. Thus both valence extrapolations are relatively short. In addition, since $m_x/m_y \leq 1/2$ and $m_y \sim m_s^{\text{phys}}$, they are done in a regime where SU(2) ChPT should be valid.

We perform the chiral and continuum extrapolations in three stages. First, the valence d quark is extrapolated to m_d^{phys} , using a functional form based on NLO

TABLE III. Fit functions and quality.

fit type	fit function	Constraints	$\chi^2/\text{d.o.f}$
B1	$1 + a^2 + L_P + S_P$	2, 3, 4	1.48
B2	$B1 + a^2 L_P + a^2 S_P$	2, 3, 4, 5, 6	1.47
B3	$B1 + \alpha_s^2 + a^2 \alpha_s + a^4$	2, 3, 4, 7, 8, 9	1.47
B4	$B2 + \alpha_s^2 + a^2 \alpha_s + a^4$	2, 3, ..., 9	1.47
N1	same as B1	none	1.91

SChPT, although including higher-order analytic terms. Details are as in Ref. [2]. This “X-fit” is done separately on each ensemble, using a correlated fit with Bayesian priors. We correct for non-analytic contributions from taste breaking in valence and sea pions and from the unphysical value of m_ℓ using the one-loop chiral logarithms (which are predicted without unknown constants). This correction depends on the ensemble, and ranges in size from 3 – 5%. The X-fits on all the new ensembles are very similar to those displayed in Refs. [2, 6, 7].

The second stage, or “Y-fit”, is the extrapolation from our three values of m_y to m_s^{phys} . The dependence on m_y is expected to be analytic, and we find that a linear fit works well. Examples of such fits are shown in Ref. [6]; those on the new ensembles are very similar.

The third and final extrapolation is that in m_ℓ , m_s and a^2 . Here we improve on Refs. [2, 6] both by having a larger range of lattice parameters and by doing these extrapolations simultaneously. As in these earlier works, we find that we cannot obtain good fits if we include results from the coarse lattices and so exclude them.

We now describe the fit functions and fitting approach used in the simultaneous chiral-continuum extrapolation. Our first fit function assumes that the lattice operator is perfectly matched to that in the continuum. Then SU(2) SChPT at NLO predicts a linear residual dependence on m_ℓ and a^2 (after taste-breaking in the chiral logarithms has been removed by hand). The only constraint on the m_s dependence is that it must be analytic, but for our short interpolation or extrapolation it is likely to be well described by a linear dependence. The appropriate fit function is thus

$$f_1(a^2, L_P, S_P) = c_1 + c_2(a\Lambda_Q)^2 + c_3 \frac{L_P}{\Lambda_X^2} + c_4 \frac{S_P}{\Lambda_X^2}, \quad (2)$$

where we are using L_P and S_P as stand-ins for m_ℓ and m_s , respectively. Taking $\Lambda_Q = 0.3$ GeV and $\Lambda_X = 1.0$ GeV (i.e. respectively a typical QCD scale and chiral expansion scale) we expect $c_2 - c_4 = \mathcal{O}(1)$. We stress that Eq. (2) is only valid for a small range of S_P around the physical value. In particular, the linear dependence on S_P is not assumed or expected to remain valid down to $S_P = 0$, and there is no *a priori* expectation that $c_4 \approx c_3$. The latter relation would only hold were we in the regime where SU(3) ChPT at NLO was valid.

When using the form f_1 we either apply Bayesian constraints, $c_i = 0 \pm 2$, to c_2 , c_3 and c_4 (fit B1) or leave all four coefficients free (fit N1). We consider the range

TABLE IV. Parameters of representative fits.

fit type	c_1	c_2	c_3	c_4	
B1/N1	0.542(7)	0.7(3)	-0.17(1)	0.00(1)	
B4	0.54(1)	0.3(4)	-0.17(2)	-0.00(2)	
fit type	c_5	c_6	c_7	c_8	c_9
B4	-0.2(8)	0.2(1)	0.1(2)	0.1(2)	0.01(3)

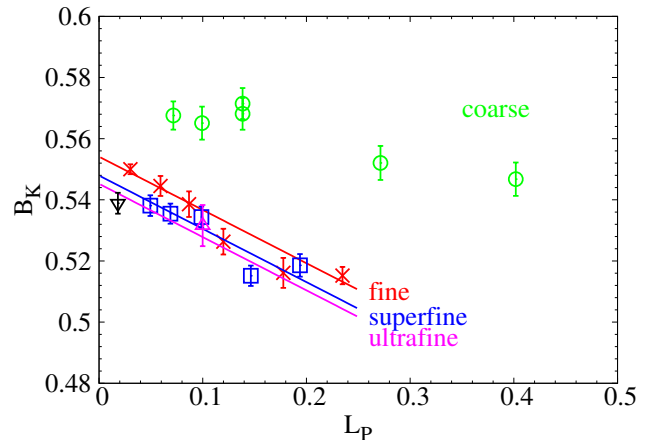


FIG. 1. $B_K(2 \text{ GeV, NDR})$ vs. $L_P (\text{GeV}^2)$, with the B1 fit. The N1 fit is indistinguishable. The result of the extrapolation is shown by the (black) triangle. The fit function for the superfine ensembles is plotted using the average values of a^2 and S_P , while for the fine ensembles the average of the values on ensembles $F1$, $F2$ and $F4$ is used. Coarse lattice results are shown for comparison; they are not included in the fit. Results from ensembles $F6$ and $F7$ are not shown (as explained in the text), but are included in the fit.

± 2 to be a fairly conservative choice for the constraints. These details, along with the resulting quality of fit, are collected in Table III. The parameters of both fits turn out to be almost identical and are given in Table IV. Both fits are reasonable, with the sizes of the constrained coefficients $c_2 - c_4$ well within the expected range of ± 2 . Thus the constraints are not important for this fit.¹

The quality of the resulting fit is illustrated by Fig. 1. A complication in displaying the fit is that within the fine ensembles there is a range of values of a^2 and S_P (and similarly for the superfine ensembles) and this feature cannot be displayed in a two-dimensional plot. The fit lines shown are for average values of a^2 and S_P , and, even with a perfect fit, would not pass exactly through the corresponding points. As can be seen from Table II, this is a small effect except for ensembles $F6$ and $F7$, which have significantly smaller values of S_P . Thus these two ensembles are not included in the figure (although they are included in the fit itself). The results on the

¹ Despite having almost identical fit parameters, the $\chi^2/\text{d.o.f}$ values for the two fits differ because in a Bayesian fit one augments both χ^2 and the effective number of data points [16].

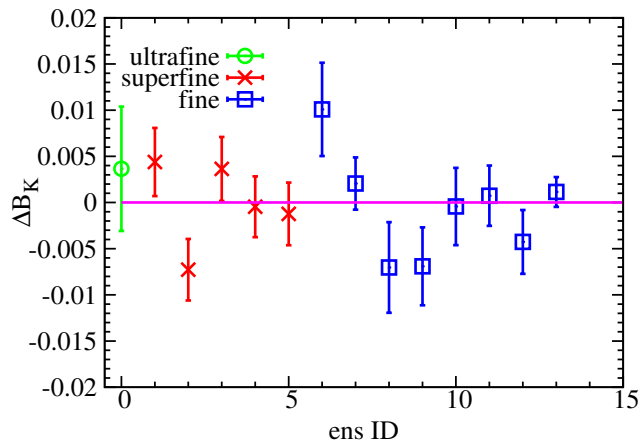


FIG. 2. Residuals ΔB_K for fit B1. The superfine lattices are ordered by decreasing L_P (S3, S4, S1, S2 and S5), while the fine lattices are ordered F6, F4, F3, F1, F5, F2, F7 and F9. These are the orders used in Tables I and II.

coarse ensembles are also shown, although they are not included in the fit. It is clear that the slope versus L_P is significantly different on the coarse ensembles, and also that there are large discretization errors. These are the features that make fits including the coarse ensembles unstable, as high order terms are needed to include them.

The complication of having different values of a^2 and S_P can be avoided by considering the residuals $\Delta B_K(i) = B_K(i) - f_1(i)$, where i labels the ensembles. These are shown in Fig. 2.

As already noted, the values of the parameters $c_2 - c_4$ lie in the expected range. In particular, if one writes the c_1 and c_2 terms in the form $c_1[1 + (a\Lambda)^2]$ then we find $\Lambda \approx 350$ MeV, which is a reasonable scale for a discretization error. We also note that the SU(3) symmetry relation $c_3 = c_4$ does not hold. Indeed, we find no significant dependence on S_P in the vicinity of the strange quark mass.

We now turn to our other fits. SU(2) SChPT is a joint expansion in a^2 and L_P (ignoring possible factors of α multiplying a^2), so at NNLO we expect a term of the form $c_5(a\Lambda_Q)^2(L_P/\Lambda_\chi^2)$ with coefficient $c_5 \sim \mathcal{O}(1)$. In fit B2 we include this term, as well as its SU(3) counterpart $c_6(a\Lambda_Q)^2(S_P/\Lambda_\chi^2)$, with coefficients constrained as for $c_2 - c_4$. In this case we find that the constraints are needed to obtain sensible fits. The resulting fit, however, lies very close to B1, and, as shown in Table III, does not have an improved $\chi^2/\text{d.o.f.}$. This simply reflects the fact that our data has similar slopes versus L_P on the fine and superfine lattices.

We next consider the impact of operator matching errors on the fit function. Since we use one-loop matching,² these errors are proportional to α^2 (with α evaluated as the scale $1/a$). Thus we also consider fits with a

$c_7\alpha^2$ term, as well as terms $c_8(a\Lambda_Q)^2\alpha$ and $c_9(a\Lambda_Q)^4$ arising from higher-order discretization errors. When adding these terms we find that Bayesian constraints (for which we use $c_7 - c_9 = 0 \pm 2$) are needed for stable fits. We have considered both fits in which only these three terms are added to f_1 (fit B3) and in which all the terms described above are included (fit B4). The full list of fits we use is shown in Table III.

We find again that adding higher-order terms does not improve the quality of the fits (see Table III), and also has little impact on the resulting fit parameters. For example, as shown in Table IV, the terms common between fits B1/N1 and B4 are almost identical, while the extra terms in B4 are all small and consistent with zero.

In summary, our data can be described well by the simple form f_1 , but is also consistent with the extra terms as long as they have small coefficients. In light of this, we have not extended the fits to include the other possible NNLO terms, e.g. that proportional to L_P^2 . We also conclude that it is reasonable to use fit B1 for our central value, while quoting the maximum difference between the results from B1 and {B2, B3, B4} fits (which turns out to be for fit B4) as an extrapolation systematic.

IV. ERROR BUDGET

We present the error budget in Table V. The largest error is from using one-loop matching, which we estimate to be $\Delta B_K/B_K = \alpha^2$, with α evaluated at scale $1/a$ for the ultrafine lattice. This error is unchanged from Ref. [2]. In principle, one can determine the size of the α^2 contribution from the chiral-continuum fit, given a sufficiently extensive set of lattice ensembles. Indeed, this term is included in fit B4 (with coefficient c_7). However, it is clear from the results of the previous section that we do not have enough ensembles to pin down c_7 , especially given the large number of parameters in the fit. Thus, although fit B4 finds a small value, $c_7 = 0.1(2)$, we do not think this is sufficiently reliable to take at face value, and prefer the conservative approach of taking $c_7 = \pm 1$ to estimate the matching error.

The errors from continuum and sea-quark mass extrapolations have been significantly reduced compared to Ref. [2]. Previously, these errors were separate, and were estimated to be 1.9% from the continuum extrapolation, 1.5% from the am_ℓ extrapolation, and 1.3% from the am_s extrapolation [2]. The combined error was thus 2.8%. The addition of the new ensembles and the use of a combined extrapolation has reduced this error to 0.9%.

only those lattice four-fermion operators composed of bilinears having the same taste as the external pions [6], Thus there are matching corrections proportional to α . These, however, appear only at NNLO in SU(2) SChPT [6], and are of the form αa^2 or αL_P . Furthermore, the numerical coefficients of these terms are small [8]. Thus we choose to treat them as effectively of NNNLO, and do not include them in the fits.

² In fact, we do not do a complete one-loop matching, since we keep

The statistical error is essentially unchanged from Ref. [2]. As in that work, we have not accounted for the impact of auto-correlations. We do observe about a 20% increase in the statistical error due to auto-correlations, as reported in Ref. [17]. However, since there is significant uncertainty in the size of this increase, and since this effect is much smaller than our current systematic errors, we have decided to neglect it in this paper.

The error from the X-fits is estimated similarly to the approach used in Ref. [2], namely by considering the effects of doubling the Bayesian priors and of switching to the eigenvalue-shift method of fitting [18]. We find that neither of these changes lead to statistically significant shifts in B_K on any ensemble. If we combine the two fractional shifts in quadrature we find an $\approx 0.1 \pm 0.1\%$ shift on essentially all fine and superfine ensembles.³ We thus take this as our estimate of this (very small) effect.

The error in Y-fits arises from the uncertainty in the functional form used to extrapolate in the valence strange-quark mass, m_y . We have used linear fits for our central value, but cannot rule out a small quadratic component. Thus we have repeated the entire analysis using quadratic Y-fits, finding a statistically significant 2.0% downward shift in the final value of B_K . This we quote as the corresponding systematic error. This error is much larger than that quoted in Ref. [2], but we think the present estimate is both more conservative and more reliable.

The finite-volume error is estimated as in Refs. [2, 19]. For our central value we do the X-fits with SChPT expressions including the (analytically known) finite-volume corrections to the chiral logarithms. We then repeat the entire analysis using infinite-volume chiral logarithms in X-fits, and take the difference between the resulting values of B_K as an error estimate. The rationale for this choice is that one-loop chiral logarithms typically provide only a semi-quantitative estimate of the size of finite-volume effects. The resulting error is numerically small.

The final two errors are those due to uncertainty in the choices of scale and of the appropriate value of the pion decay constant to use in the chiral logarithms entering X-fits. We follow the MILC collaboration and set the scale using $r_1 = 0.3117(22)$ fm [20]. To obtain our central value of B_K we take $r_1 = 0.3117$. We then repeat the analysis on each ensemble using both $r_1 = 0.3139$ and 0.3095. We find that both changes lead, on all fine, superfine and ultrafine ensembles, to shifts of magnitude $\approx 0.3\%$ in B_K . Given this uniformity, we expect a similar shift in the final answer and thus take this as our error estimate.

For the decay constant we use $f_\pi = 132$ MeV (a somewhat outdated approximation to the physical value of

TABLE V. Error budget for B_K using SU(2) SChPT fitting.

cause	error(%)	memo
STATISTICS	0.64	jackknife
matching factor	4.4	see text
$\left. \begin{array}{l} \text{discretization} \\ am_\ell \text{ extrap} \\ am_s \text{ extrap} \end{array} \right\}$	0.9	diff. of B1 and B4 fits
X-fits	0.1	see text
Y-fits	2.0	diff. of linear and quad.
finite volume	0.4	diff. of $V=\infty$ and FV fit
r_1	0.3	r_1 error propagation
f_π	0.1	132 MeV vs. 124.4 MeV
TOTAL SYSTEMATIC	4.9	

130.41 MeV) for determining the central value of B_K , and then repeat the analysis using the decay constant in the SU(2) chiral limit, $f_\pi^{(0)} = 124.2$ MeV [9]. This is the same procedure as in Refs. [2, 6]. In this case the shift in B_K does vary significantly between ensembles, so we repeat the entire analysis using both values of f_π , and take the difference in final values as our estimate of the error. As the Table shows, the resulting error is very small.

V. CONCLUSION

Our final results are

$$B_K(2 \text{ GeV, NDR}) = 0.5388 \pm 0.0034 \pm 0.0266 \quad (3)$$

$$\hat{B}_K = 0.7379 \pm 0.0047 \pm 0.0365 \quad (4)$$

where the first errors are statistical and the second systematic. $\hat{B}_K = B_K(\text{RGI})$ is the renormalization group invariant value of B_K . This result supersedes our previous result, $\hat{B}_K = 0.727 \pm 0.004 \pm 0.038$ [2], with which it is completely consistent. Although the changes are numerically small, they are significant. By adding many new ensembles we now can properly extrapolate in sea quark masses (rather than estimate the effect of such an extrapolation and include it as an error). This is the main reason for the small increase in the central value. It also leads to a significant reduction in the systematic errors from the continuum and sea-quark mass extrapolations. On the other hand, a more careful estimate of the systematic error in the valence strange-quark mass extrapolation has led to a significant increase in this error. All told, the overall error is only slightly reduced, but, more importantly, the methods of estimating errors have been improved.

Our result (4) is consistent with the world average presented in Ref. [5], $\hat{B}_K = 0.766(10)$. Our error is larger than this average primarily because of our use of one-loop matching factors. We are presently working on obtaining the matching factors using non-perturbative renormalization [21], which should result in substantial reduction of

³ The combined shift is $0.4 \pm 0.5\%$ on the U1 ensemble. The larger error is due to our smaller number of measurements on this ensemble.

the matching error[22, 23]. In addition, we plan to calculate the matching factors perturbatively at the two-loop level using automated perturbation theory.

Our second-largest error is that from Y-fits. This error can, however, be essentially removed in a straightforward way by using valence strange quarks tuned to the physical value.

ACKNOWLEDGMENTS

We are grateful to Claude Bernard and the MILC collaboration for private communications. C. Jung is supported by the US DOE under contract DE-AC02-

98CH10886. The research of W. Lee is supported by the Creative Research Initiatives program (2013-003454) of the NRF grant funded by the Korean government (MSIP). W. Lee would like to acknowledge the support from KISTI supercomputing center through the strategic support program for the supercomputing application research [No. KSC-2012-G2-01]. The work of S. Sharpe is supported in part by the US DOE grant no. DE-FG02-96ER40956. Computations for this work were carried out in part on QCDOC computers of the USQCD Collaboration at Brookhaven National Laboratory and in part on the DAVID GPU clusters at Seoul National University. The USQCD Collaboration are funded by the Office of Science of the U.S. Department of Energy.

-
- [1] R. Arthur *et al.* (RBC Collaboration, UKQCD Collaboration), Phys.Rev. **D87**, 094514 (2013), arXiv:1208.4412 [hep-lat].
 - [2] T. Bae, Y.-C. Jang, C. Jung, H.-J. Kim, J. Kim, *et al.*, Phys.Rev.Lett. **109**, 041601 (2012), arXiv:1111.5698 [hep-lat].
 - [3] S. Durr, Z. Fodor, C. Hoelbling, S. Katz, S. Krieg, *et al.*, Phys.Lett. **B705**, 477 (2011), arXiv:1106.3230 [hep-lat].
 - [4] C. Aubin, J. Laiho, and R. S. Van de Water, Phys.Rev. **D81**, 014507 (2010), arXiv:0905.3947 [hep-lat].
 - [5] S. Aoki, Y. Aoki, C. Bernard, T. Blum, G. Colangelo, *et al.*, (2013), arXiv:1310.8555 [hep-lat].
 - [6] T. Bae, Y.-C. Jang, C. Jung, H.-J. Kim, J. Kim, *et al.*, Phys.Rev. **D82**, 114509 (2010), arXiv:1008.5179 [hep-lat].
 - [7] T. Bae, Y.-C. Jang, H. Jeong, J. Kim, J. Kim, *et al.*, PoS, 476 (LATTICE 2013), arXiv:1310.7319 [hep-lat].
 - [8] J. Kim, W. Lee, and S. R. Sharpe, Phys.Rev. **D83**, 094503 (2011), arXiv:1102.1774 [hep-lat].
 - [9] A. Bazavov, D. Toussaint, C. Bernard, J. Laiho, C. DeTar, *et al.*, Rev.Mod.Phys. **82**, 1349 (2010), arXiv:0903.3598 [hep-lat].
 - [10] A. Hasenfratz and F. Knechtli, Phys. Rev. **D64**, 034504 (2001), arXiv:hep-lat/0103029 [hep-lat].
 - [11] C. Bernard, private communications (2009-13).
 - [12] C. Davies, E. Follana, I. Kendall, G. P. Lepage, and C. McNeile (HPQCD Collaboration), Phys.Rev. **D81**, 034506 (2010), arXiv:0910.1229 [hep-lat].
 - [13] W.-J. Lee and S. R. Sharpe, Phys.Rev. **D60**, 114503 (1999), arXiv:hep-lat/9905023 [hep-lat].
 - [14] C. Aubin and C. Bernard, Phys.Rev. **D68**, 034014 (2003), arXiv:hep-lat/0304014 [hep-lat].
 - [15] R. S. Van de Water and S. R. Sharpe, Phys. Rev. **D73**, 014003 (2006), arXiv:hep-lat/0507012.
 - [16] G. Lepage, B. Clark, C. Davies, K. Hornbostel, P. Mackenzie, *et al.*, Nucl.Phys.Proc.Suppl. **106**, 12 (2002), arXiv:hep-lat/0110175 [hep-lat].
 - [17] B. Yoon, T. Bae, H.-J. Kim, J. Kim, J. Kim, *et al.*, PoS **LAT2009**, 263 (2009), arXiv:0910.5581 [hep-lat].
 - [18] B. Yoon, Y.-C. Jang, C. Jung, and W. Lee, J.Korean Phys.Soc. **63**, 145 (2013), arXiv:1101.2248 [hep-lat].
 - [19] J. Kim, C. Jung, H.-J. Kim, W. Lee, and S. R. Sharpe, Phys.Rev. **D83**, 117501 (2011), arXiv:1101.2685 [hep-lat].
 - [20] A. Bazavov *et al.* (Fermilab Lattice Collaboration, MILC Collaboration), Phys.Rev. **D85**, 114506 (2012), arXiv:1112.3051 [hep-lat].
 - [21] G. Martinelli, C. Pittori, C. T. Sachrajda, M. Testa, and A. Vladikas, Nucl. Phys. **B445**, 81 (1995), arXiv:hep-lat/9411010 [hep-lat].
 - [22] J. Kim, B. Yoon, and W. Lee, PoS **LATTICE2012**, 241 (2012), arXiv:1211.2077 [hep-lat].
 - [23] A. T. Lytle and S. R. Sharpe, (2013), arXiv:1306.3881 [hep-lat].